IOMAC'15
6th International Operational Modal Analysis Conference
2015 May12-14 Gijón - Spain

COMPARATIVE STUDY OF OMA APPLIED TO EXPERIMENTAL AND SIMULATED DATA FROM AN OPERATING VESTAS V27 WIND TURBINE

Oscar Ramírez [1], *Dmitri Tcherniak* [2], *and Gunner Chr. Larsen* [3]

[1] Research Assistant, DTU Wind Energy, Technical University of Denmark, orre@dtu.dk
[2] Research Engineer, Brüel & Kjær Sound and Vibration Measurement, dmitri.tcherniak@bksv.com
[3] Senior Scientist, DTU Wind Energy, Technical University of Denmark, gula@dtu.dk

ABSTRACT
Today, design of wind turbines is extensively done by the implementation of numerical models. These models simulate the dynamic behaviour of full-scale wind turbines which helps to ensure the structural integrity of prototypes. However, these numerical models need validation from experimental results, and in turn, numerical and analytical modelling help improve and validate new experimental techniques. Wind turbines are complex dynamic systems that consist of mutually moving substructures under high dynamic loads. At a standstill, the system can be modelled as linear time-invariant (LTI), and modal analysis requirements are thus fulfilled for the dynamic characterization. Under operation, the system cannot be considered as LTI and must be modelled as a linear periodic time-variant (LPTV) system, which allows for the application of the related theory for such systems. One of these methods is the Coleman transformation, which transforms the vibrations expressed in the blade rotating coordinates to the fixed-ground frame of reference. The application of this transformation, originally from helicopter theory, allows for the conversion of a LPTV system to a LTI system under certain assumptions, among which is the assumption of isotropic rotors. Since rotors are never completely isotropic in real life, this paper presents the application of operational modal analysis together with the Coleman transformation on both experimental data from a full-scale Vestas wind turbine with instrumented blades and nacelle, and its representative numerical model with a fully isotropic rotor. The results show that the first tower and rotor edgewise modes are well identified, and that the rotor edgewise modes can be identified from the nacelle signals. The results also uncover the challenge the excitation forces imply for the identification of flapwise modes.

Keywords: wind turbines, structural dynamics, operational modal analysis, modal parameters, system identification, anisotropic rotors

1. INTRODUCTION

Cost of Energy (CoE) reduction is the main driver for the increase of wind turbine size. As the size grows, higher dynamic loads and response magnitudes may occur, which can decrease the lifetime of the wind turbine. Therefore, designers are required to understand wind turbine dynamics to succeed in obtaining a better balance between materials, performance and cost. The dynamic characterization is generally done in terms of modal parameters - modal frequencies, damping and mode shapes - where a proper estimation is essential, for instance, to avoid inconvenient cases such as coupling of modal frequencies with multiples of the rotational speed, or to predict the fatigue loads from which the structure suffers. This paper presents the findings obtained in [1], where the identification of modal parameters was performed on measurements from a full-scale Vestas V27 (hereafter, V27) wind turbine. Despite the fact that the V27 is an old wind turbine, its design is similar to modern wind turbines, as it features pitch- and yaw-control. The focus is on the frequency range 0-5 Hz, which includes the lowest global modes.

1.1. OMA on Wind Turbines

Wind turbines are huge structures, subjected to stochastic loading distributed over a substantial part of the structure, and therefore, Operational Modal Analysis (OMA) techniques sparked the interest of industry and academia because of the advantages of identifying modal properties based on response-only while operating. However, an operating wind turbine may violate some OMA assumptions, and some approximations must be made to apply OMA with a certain level of confidence. From the different algorithms OMA embraces, the Stochastic Subspace Identification (SSI) technique, described by Overschee and De Moor [2], seems the most applicable based on the success of previous research studies. In the present work, a commercial software package from Brüel & Kjær is used in which this method is already implemented.

1.2. State of the Art

The theoretical basis of this work was mainly laid by Hansen [3, 4], whose work describes the Coleman transformation and its main assumptions in depth; Bir [5], who developed a new Coleman transformation scheme, extending its applicability limit; and Skjoldan [6], who compared the Floquet and Hill methods for anisotropic rotors with the Coleman transformation for isotropic rotors. Recently, Mevel et al. developed a new subspace algorithm for the modal analysis of rotating systems and applied it to helicopter rotors [7]. Yang et al.[8] applied another method based on the extension of modal analysis to LPTV systems, the harmonic power spectrum (HPS), and made a comparison with the Coleman transformation followed by SSI using the blade accelerations of an operating Vestas V27. The latter concluded the Coleman transformation could lead to erroneous results due to rotor anisotropy.

To the authors' knowledge, there are only few research studies involving modal analysis of operating wind turbines. Tcherniak and Larsen [9] presented a full-scale study including blade instrumentation and data acquisition, the processing of data to convert the system to LTI and assessed preliminary results using parked, idling and normal operation cases of a Vestas V27. Di Lorenzo et al. [10] also used the Coleman transformation for modal identification of a Micon 65/13M. Further, Hansen et al. [11] estimated the aeroelastic damping of a NM80 2.75 MW operating prototype using strain gauges. They concluded that the SSI method can handle deterministic excitation from wind, and the first tower and rotor edgewise whirling modes could be identified. Tcherniak et al. applied SSI to an operating ECO 100 Alstom using accelerometers on the nacelle and tower, identified some rotor modes using only these signals, and produced experimental Campbell diagrams based on 4 months of measurements [12]. Van Der Valk and Ogno [13] identified the first four global eigenfrequencies in an idling Siemens offshore SWT-3.6 MW turbine using several strain gauges and one accelerometer, with the best results coming from the accelerometer.

1.3. Motivation

The main motivation of this work was to investigate how reliable the application of the Coleman transformation [14] is when comparing anisotropic and isotropic rotors. Other ideas to explore were: if modes could be identified using only the nacelle sensors and if flapwise modes could be identified successfully, since there is a lack of research regarding these modes. This research was performed on experimental data, as well as on its equivalent numerical model, implemented in the nonlinear aeroelastic code HAWC2. Both identification results were assessed against theoretical predictions from the linear aeroelastic stability tool HAWCStab2.

2. WIND TURBINE MODAL DYNAMICS

The dynamics of wind turbines are composed of three main substructures: tower, drivetrain and rotor. The tower deflects longitudinally and laterally with respect to the wind direction, where these two bending modes interact due to the gyroscopic coupling of the towertop and rotor. Also, the tower torsion couples to the yaw motion of the nacelle and rotor. The drivetrain facilitates the blades to rotate around its axis: taking one blade as reference, the azimuth angle is the angular position of that blade. The drivetrain consists of a main shaft, a gearbox and a generator, and introduces a torsional mode between the rotor hub and generator coupled with the blade's simultaneous edgewise bending (or flapwise bending, depending on the pitch angle). A single blade cantilevered at the hub has three mode families: flapwise, edgewise and torsion. It is difficult to find pure representatives of these families because the modes are typically a mixture of them.

2.1. Rotor Dynamics

The term rotor is understood as the assembly of blades attached to a hub. For each mode of a single blade, one can find three modes of the rotor: one symmetric - all blades deflect symmetrically - and two asymmetric - two blades deflect contrary to the remaining blade, as illustrated in Figure 1.

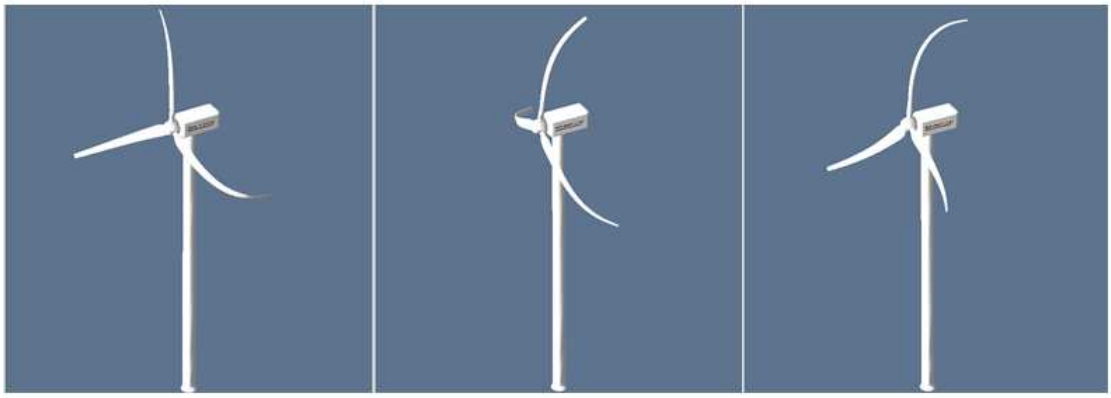

Figure 1: Components of the first flapwise mode

When the rotor starts rotating, the natural frequencies of the rotor modes change. The centrifugal stiffening can only partly explain this phenomenon. The qualitative change from LTI (when the rotor is not rotating) to LPTV system (when rotating) is the main reason of the major changes in dynamics. The modes of the LPTV system consist of components (known from the Floquet analysis as the Fourier components); the frequencies of these components are separated by the multiples of the rotational frequency Ω. This explains the separation of the backward (BW) and forward (FW) whirling components of the modes, which is typically illustrated by the Campbell diagram (e.g. Figure 2). Further details about the rotor dynamics are described in [3].

2.2. The Coleman Transformation

At a standstill, the system can be considered as LTI and all OMA assumptions are fulfilled. But when the wind turbine is under operation, the system is not LTI any more, and traditional modal analysis cannot be directly applied. The Coleman transformation, also known as multiblade coordinate transformation (MBC), converts the rotating blade coordinates to the non-rotating frame, transforming the system from LPTV to LTI. For a 3-bladed rotor, with the blades equally spaced, MBC is defined as

$$a_0 = \frac{1}{3}\sum_{k=1}^{3} q_k \qquad a_1 = \frac{2}{3}\sum_{k=1}^{3} q_k \cos\psi_k \qquad b_1 = \frac{2}{3}\sum_{k=1}^{3} q_k \sin\psi_k \tag{1}$$

where $\psi_k = \Omega t + \frac{2\pi}{3}(k-1)$ is the azimuth angle of blade $k = 1, 2, 3$. The three multiblade coordinates a_0, a_1 and b_1 replace the blade coordinates q_1, q_2 and q_3, measuring the same degree of freedom (DOF) on blade k, respectively. The inverse transformation back to the blade coordinates is

$$q_k = a_0 + a_1 \cos\psi_k + b_1 \sin\psi_k \tag{2}$$

The transformed blade coordinates in the non-rotating frame can be categorized in one symmetric a_0 (collective) and two asymmetric components a_1 and b_1. For instance, if one assumes a flapwise deflection (aligned with the wind direction) of the blade coordinates q_k, a_0 will describe all blades deflecting symmetrically, while a_1 and b_1 will describe the FW and BW whirling motions, respectively (cf. Figure 1). This transformation results in a linear eigenvalue problem for which a solution defines a mode of the wind turbine. The mathematical derivation is detailed in [3].

3. EXPERIMENTAL DATA

The complete description of the conducted measurement setup to collect the experimental data can be found in [9], including details regarding equipment and challenges involving the instrumentation of the turbine. For the sake of simplicity, the information here just relates to the signals involved in the analysis.

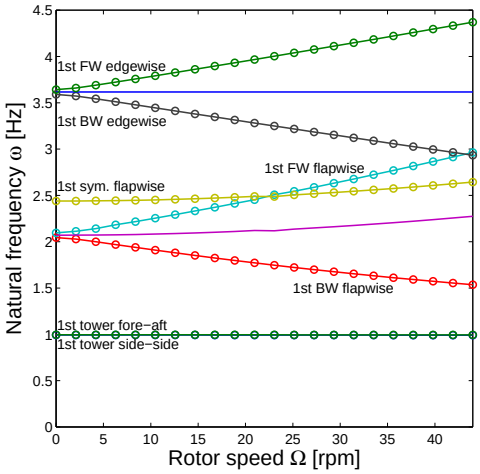

Figure 2: Campbell diagram for the V27

3.1. Selection of Signals

Though each blade was instrumented with 12 accelerometers (10 in the flap- and 2 in the edgewise direction) only 4 signals per blade were selected for the present analysis. The corresponding sensors were located at 96% and 67% of the blade span, respectively. The reasoning behind this choice was firstly that these sensors are assumed sufficient to represent with confidence the lowest modes in the 0-5 Hz range and secondly to reduce the risk of misalignment by using sensors forming a 90° angle between them. The nacelle was instrumented with triaxial accelerometers targeted to identify not only the tower modes, but also the rotor modes, as Tcherniak et al. showed in [12].

3.2. Selection of Data Sets

A wind turbine may be modelled as an LPTV system, if the fluctuation of variables such as rotor speed, blade pitch and nacelle yaw is minimal. For this reason, the data set selection was based on a low standard deviation of these parameters. OMA requires a long time series for better performance of the algorithm, and here 20 minutes were believed to represent a good trade-off between computational time and the OMA data amount requirement. In addition, the V27 control system can only run the turbine at low and

high rotor speed (Ω_{low}, Ω_{high}), approximately at 33 rpm and 43 rpm. Providing these considerations, two data sets are selected for detailed analysis. The wind excitation in the HAWC2 model was based on meteorological data from the selected time spans. Table 1 shows details from the selected data sets, including the relevant standard deviations on which their selection was based, and descriptive mean variables. The latter are compared to those obtained from the HAWC2 simulations in Table 2, and to the operational data used in HAWCStab2 in Table 3. It can be noticed that the HACWStab2 operational data does not match perfectly for neither the high rotor speeds - leading to issues in the identification of modal frequencies - nor the mean pitch angle - leading to issues in the extracted damping ratios.

Parameter	Ω_{low}	Ω_{high}
Date	16/12/12	15/12/12
Time	11:10-11:30	05:10-05:30
Std. Dev. tacho	0.54 rpm	1.28 rpm
Std. Dev. pitch	0.09°	0.59°
Std. Dev. yaw	0.17°	0.02°
Std. Dev. wind speed	0.56 m/s	1.37 m/s
Max./min. power	0/0 kW	265/56.3 kW
Mean rotor speed	32.20 rpm	43.10 rpm
Mean wind speed	5 m/s	11 m/s
Mean pitch angle	0°	0.67°

Table 1: Details of data sets

Parameter	Ω_{low}	Ω_{high}
Mean rotor speed	32.24 rpm	43.22 rpm
Mean wind speed	5 m/s	11 m/s
Mean pitch angle	0°	0.74°

Table 2: HAWC2 modelling details

Parameter	Ω_{low}	Ω_{high}
Mean rotor speed	32.14 rpm	35.02 rpm
Mean wind speed	5 m/s	11 m/s
Mean pitch angle	0.41°	1.57°

Table 3: HAWCStab2 modelling details

4. SIMULATION VS. EXPERIMENT

The dynamic behaviour of the V27 was simulated using the aeroelastic code HAWC2 [15], intended for calculating wind turbine response in the time domain. HAWC2 can provide output channels to simulate the biaxial blade and triaxial nacelle acceleration sensors on the V27. The theoretical modal analysis is performed in HAWCStab2 [16], which predicts structural and aeroelastic modal frequencies, damping ratios and mode shapes, through open- and closed-loop aero-servo-elastic eigenvalue and frequency-domain analysis. Although the structural part of the two codes use the same beam element (Timoshenko), the kinematics of the codes are different. HAWC2 is based on a multi-body formulation, while HAWCStab2 is based on a co-rotational formulation. Figure 3 shows the predicted structural and aeroelastic modal frequencies and damping ratios during the entire operational range, from which results at 5 m/s and 11 m/s wind speed, respectively, corresponding to the selected data sets, were analysed for comparison.

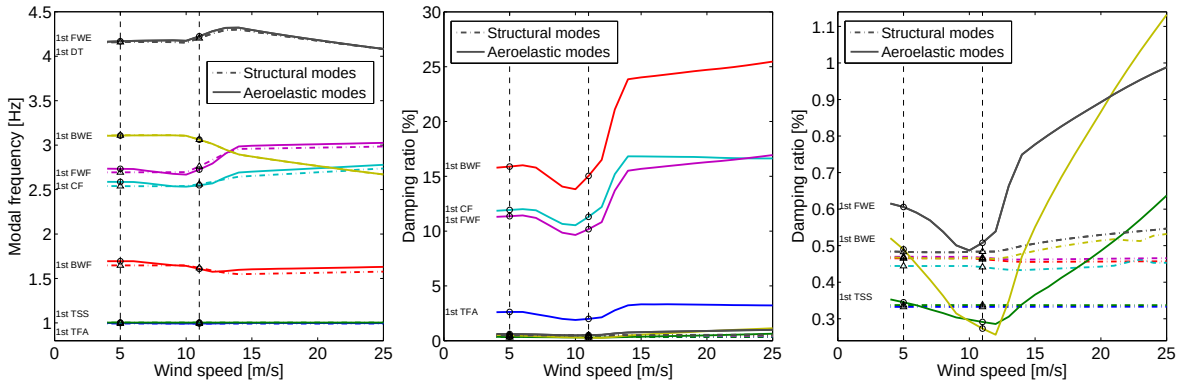

(a) Modal frequencies **(b)** Modal damping ratios **(c)** Low damped modes

Figure 3: Predicted frequencies and damping ratios at Ω_{low} and Ω_{high} (5 m/s and 11 m/s)

Figure 4 shows the Power Spectral Density (PSD) from the nacelle and blade signals used to validate

the simulations against the experiment. A fairly good agreement is observed in Figure 4 (b,c), where besides the rotor harmonics, a peak is present between 6P and 7P. This could refer to an edgewise mode based on the previous theoretical predictions. However, the experimental data features a double-peak phenomenon that is inconsistent with the isotropic case and might refer to the effect of rotor anisotropy.

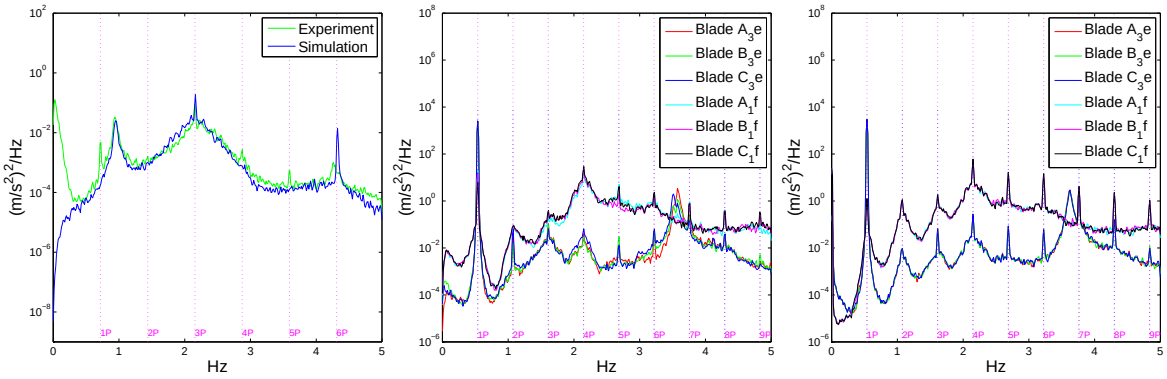

(a) Tower fore-aft signals at Ω_{high} **(b)** Blade experimental data at Ω_{low} **(c)** Blade simulated data at Ω_{low}

Figure 4: PSD of nacelle and outer section blades signals. Subscripts *1* and *3* denote flapwise and edgewise

5. SIGNAL ANALYSIS

Prior to the application of OMA, a natural step is to apply signal analysis, since this is not based on any assumptions and thus not prone to violate OMA assumptions. A singular value decomposition (SVD) is performed on the blade signals to get more information about the peak between 6P and 7P, according to Figure 5 (a,b).

Apparently, two singular vectors are required to describe that peak, and therefore, very likely unveil two modes at this frequency rather than one. Figure 5 (c,d) illustrates the application of the MBC to the blade signals, which gives indeed two peaks separated by 2Ω, thus suggesting the edgewise whirling components. The characteristic double peak in the experimental data is still present, but also the 3P and multiple harmonics are not removed in the isotropic case. This is contrary to the experimental data, where the rotor is anisotropic. The flapwise analysis does not give any useful information prior to modal identification - reinforcing the statement formulated in [17], where the operational forces (aerodynamic loads) pose a challenge, resulting in non-flat spectra at lower frequencies interfered by the rotor harmonics.

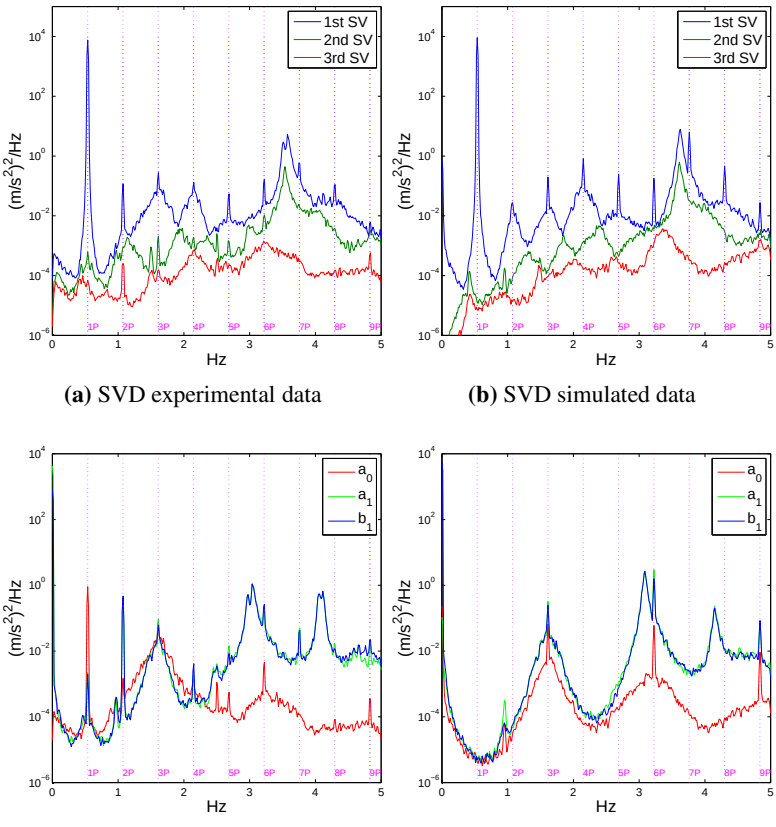

(a) SVD experimental data **(b)** SVD simulated data

(c) MBC experimental data **(d)** MBC simulated data

Figure 5: SVD and MBC applied on edgewise signals at Ω_{low}

6. MODAL IDENTIFICATION

The modal identification was performed on the experimental and simulated data using OMA software Type 7760 from Brüel & Kjær. The signals were first decimated to cover the frequency range of interest, 0-5 Hz. From the 4 selected signals per blade, only those 2 at the outer section were enabled as projected channels, since they provide more relevant information. The SSI unweighted principal component (UPC) technique was then performed on the data to identify the global tower and rotor modes (edge- and flapwise). The modal parameter identification was limited to a 1.5% damping ratio for in-plane modes (tower side-side, rotor edgewise) and to 20% for out-of-plane modes (tower fore-aft, rotor flapwise), according to the HAWCStab2 results (cf. Figure 3). Hence, all modes identified with damping ratios above these thresholds are ignored. The identification was supported with animations of the modes. These animations were, in the case of tower modes, a visual representation of the entire wind turbine, whereas in the case of the rotor modes they referred to the animation of the symmetric a_0 and asymmetric components, a_1 and b_1. A collective component denotes the excited symmetric component, and an asymmetric component has two excited asymmetric components, where the phase difference indicates if it is a BW or FW component.

With the mentioned setup, the tower modes were well identified for both experimental and numerical HAWC2 cases, displaying a fine agreement among them, as can be seen in Figure 6 (a,b). The edgewise components were also identified successfully, using only the nacelle sensors. This agrees with [12], where the flapwise components could not be identified from the nacelle signals, and it was mentioned that their identification is more challenging, requiring the blades to be fitted with instruments. Actually, the flapwise components seemed to be identified around 3P, according to Figure 6 (a,b), but they could not be traced in either the PSD or the SVD analyses.

In parallel, Figure 7 shows the identified edgewise modes from the blade signals. This not only confirms the identification based on the nacelle signals, but also makes the identification much more straightforward, as compared to using nacelle sensors only.

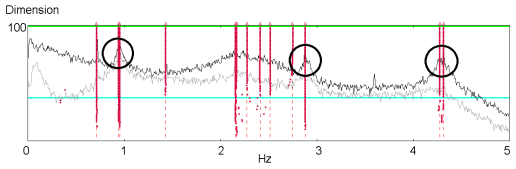

(a) Experimental data

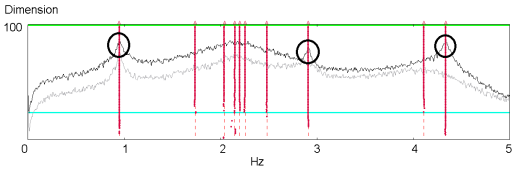

(b) Simulated data

Figure 6: Tower modes at Ω_{high}

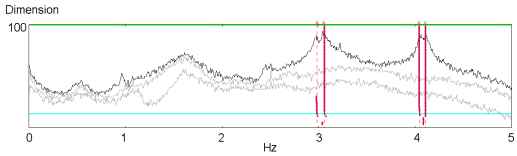

(a) Experimental data

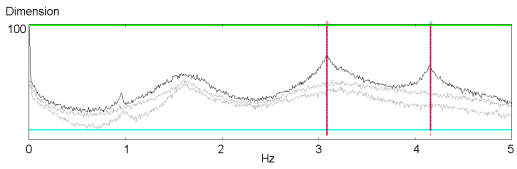

(b) Simulated data

Figure 7: Edgewise modes at Ω_{low}

6.1. Induced Rotor Anisotropy in Simulated Data

In the edgewise components, one can notice a double-peak phenomenon that might be associated with rotor anisotropy (dissimilarities in blades or difference among sensor positions/orientations). From the blade signals, Figure 7 shows that the two peaks at each component requires the algorithm to identify double modes instead of a single one. To confirm the rotor anisotropy hypothesis, a test case was implemented in the numerical model, where the stiffness of one blade was different from the other two. The results are shown in Figure 8, where the double peak is found in a similar manner as in the experimental data. Apparently, the more different the blades are, the larger the frequency difference between the two

peaks.

6.2. Identification of Flapwise Components

In contrast, the identification of flapwise components required special treatment. First, both the experimental and numerical data were analysed following the same procedure as for the edgewise modes. However, no peaks were clearly visible. Next, a band-pass filter was applied between 1.4 and 3 Hz to improve the flapwise identification results without notable success. Therefore, as an attempt to understand what makes the identification of flapwise modes so difficult, a new strategy was attempted. An artificial impulse excitation in the numerical model was introduced that was expected to better meet OMA assumptions with respect to the operational forces. The drawback of this strategy is that the excitation is not ambient any more, and that the best identification results for the flapwise components in the experimental data are linked to the aforementioned band-pass filtering. This new approach was implemented in three different versions: impulse-only excitation; wind (no turbulence) added to the impulse excitation; and wind and turbulence added to the impulse excitation. Figure 9 illustrates the three different cases tested and highlights the three flapwise components identified independently of the excitation case. It can be observed in Figure 9 (a) that the flapwise mode components are clearly visible with only the impulse excitation acting as operational forces. When the wind is introduced in Figure 9 (b), the emerging excited peaks are overlapped which complicates the identification. Despite this, the algorithm was still capable of identifying all the components.

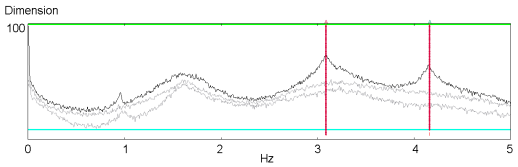

(a) Simulated data

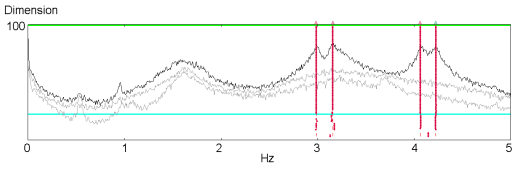

(b) Simulated data, induced anisotropy

Figure 8: Anisotropic effects at Ω_{low}

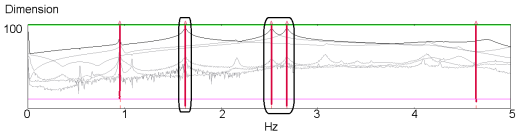

(a) Impulse only

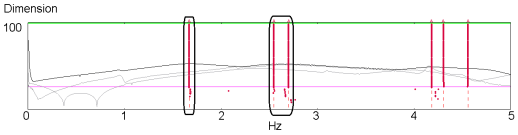

(b) Impulse + wind

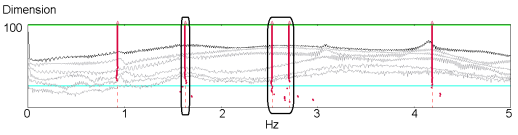

(c) Impulse + wind + turbulence

Figure 9: Flapwise components at Ω_{low}

		Frequencies [Hz]			Damping [%]		
	Mode (1st)	Experiment	Simulation	HAWCStab2	Experiment	Simulation	HAWCStab2
Ω_{low}	Tower fore-aft	0.95	0.95	0.99	1.90	2.15	2.62
	Tower side-side	0.96	0.96	1.00	1.35	1.68	0.35
	BW flapwise	1.84	1.63	1.69	10.15	11.34	15.88
	Sym. flapwise	2.63	2.54	2.59	7.00	11.05	11.92
	FW flapwise	2.79	2.71	2.73	9.30	10.91	11.36
	BW edgewise	3.04*/3.05	3.09*/3.09	3.11	1.2*/1.12	0.84*/0.61	0.49
	FW edgewise	4.11*/4.11	4.16*/4.14	4.17	1.17*/0.62	0.75*/0.91	0.61
Ω_{high}	Tower fore-aft	0.94	0.95	0.99	2.51	2.11	1.99
	Tower side-side	0.95	0.95	1.00	1.23	1.05	0.29
	BW flapwise	1.70	1.69	1.61	19.24	18.84	15.03
	Sym. flapwise	-	-	2.55	-	-	11.31
	FW flapwise	-	-	2.72	-	-	10.18
	BW edgewise	2.88*/2.87	2.91*/2.91	3.06	0.42*/0.35	0.59*/0.62	0.27
	FW edgewise	4.31*/4.33	4.34*/4.34	4.23	0.69*/0.70	0.45*/0.50	0.51

Table 4: Modal parameters comparison (*identification from nacelle sensors only)

However, an even higher impulse excitation was needed to properly identify these modes when adding the turbulence in Figure 9 (c), thus pinning down the turbulence as the major hurdle. This unexpectedly hinders the identification proportionally to the turbulence intensity, though the broad banded stochastic nature of turbulence is considered as a perfect excitation for OMA. Table 4 shows that, overall, the experimental and simulated results match well. It also displays discrepancies due to the flapwise problem mentioned above, as well as deviations in tower and edgewise modal parameters attributed to the HAWCStab2 model structural properties.

7. CONCLUSIONS

The paper presents modal identification of the lowest tower and rotor modes (except the torsional modes) of an operating V27 turbine. It was demonstrated that it is possible to extract modal parameters from experimental data by applying the MBC in conjunction with OMA SSI. The tower and rotor edgewise modes could even be extracted from the nacelle signals. However, a double peak phenomenon in the experimental data, caused by rotor anisotropy, complicated the identification of the edgewise mode components. The problem was circumvented using both the nacelle and blade signals. Using band-pass filtering, the flapwise components were also identified but with higher uncertainty. The reason of this high uncertainty is associated with the turbulence loading, resulting from a three-step numerically-based input parameter study.

ACKNOWLEDGEMENTS

EUDP (Danish Energy Technology Development and Demonstration Programme) is gratefully acknowledged for embracing the measurement campaign conducted between October 2012 and May 2013, under the project, "Predictive Structure Health monitoring of Wind Turbines", with grant number 64011-0084.

REFERENCES

[1] Ramírez, O. (2014) Identification of Modal Parameters Applying Operational Modal Analysis on a Full Scale Operating Vestas V27 Wind Turbine. *Master's thesis*, Technical University of Denmark.

[2] Van Overschee, P. and De Moor, B. (1996) *Subspace identification for linear systems: theory, implementation, applications.* Kluwer Academic Publishers.

[3] Hansen, M. H (2007) Aeroelastic instability problems for wind turbines. *Wind Energy* Vol. 10, p. 551-577.

[4] Hansen, M. H (2003) Improved modal dynamics of wind turbines to avoid stall-induced vibrations. *Wind Energy* Vol. 6, p. 179-195.

[5] Bir, G. (2008) Multiblade coordinate transformation and its application to wind turbine analysis. *ASME Wind Energy Simposium*, Reno, Nevada.

[6] Skjoldan, P. F. (2008) Modal Dynamics of Wind Turbines with Anisotropic Rotors. *Proceedings of 47th AIAA Aerospace Sciences Meeting*.

[7] Mevel, L. and Gueguen, I. and Tcherniak, D. (2014) LPTV Subspace Analysis of Wind Turbines Data. *EWSHM - 7th European Workshop on Structural Health Monitoring*.

[8] Yang S. and Tcherniak D. and Allen M. S. (2014) Modal Analysis of Rotating Wind Turbine Using Multiblade Coordinate Transformation and Harmonic Power Spectrum. *Topics in Modal Analysis I*, Vol. 7, p. 77-92, A Conference and Exposition on Structural Dynamics (Proceedings of the 32nd IMAC).

[9] Tcherniak, D. and Larsen, G. C. (2013) Application of OMA to an Operating Wind Turbine: now including Vibration Data from the Blades. *Proceedings - 5th International Operational Modal Analysis Conference (IOMAC'13)*.

[10] Di Lorenzo, E. and Manzato, S. and Peeters, B. and Marulo, F. (2014) Structural health monitoring techniques applied to operating wind turbines. *Proceedings of the 9th International Conference on Structural Dynamics*, EURODYN 2014.

[11] Hansen, M. H. and Thomsen, K. and Fuglsang, P. and Knudsen, T. (2006) Two Methods for Estimating Aeroelastic Damping of Operational Wind Turbine Modes from Experiments. *Wind Energy*, Vol. 9, p. 179-191

[12] Tcherniak, D. and Chauhan, S. and Basurko, J. and Salgado, O. and Carcangiu, C. E. and Rossetti, M. (2011) Application of OMA to Operational Wind Turbine. *Proceedings - 4th International Operational Modal Analysis Conference (IOMAC'11)*.

[13] Van Der Valk P. L. C. and Ogno M. G. L. (2014) Identifying Structural Parameters of an Idling Offshore Wind Turbine Using Operational Modal Analysis. *Dynamics of Civil Structures*, Vol. 4, p. 271-281, A Conference and Exposition on Structural Dynamics, (Proceedings of the 32nd IMAC).

[14] Coleman, R. P. and Feingold, A. M (1957) Theory of self-excited mechanical oscillations of helicopter rotors with hinged blades. *NACA Report 1351*, Langley Aeronautical Laboratory.

[15] Larsen, T. J. and Hansen, A. M. -(2013) How 2 HAWC2, the user's manual. *Ris-R-1597 (ver. 4-4)(EN)*, Technical University of Denmark.

[16] Hansen, M. H (2004) Aeroelastic stability analysis of wind turbines using an eigenvalue approach. *Wind Energy* Vol. 7, p. 133-143.

[17] Tcherniak, D. and Chauhan, S. and Hansen, M. H. (2011) Applicability Limits of Operational Modal Analysis to Operational Wind Turbines. *Structural Dynamics and Renewable Energy*, Vol. 1, Society for Experimental Mechanics, p. 317-327 (Conference Proceedings of the Society for Experimental Mechanics Series; No. 10).